AIP | Journal of Applied Physics

A computational analysis of graphene adhesion on amorphous silica

Eunsu Paek and Gyeong S. Hwang

Citation: J. Appl. Phys. **113**, 164901 (2013); doi: 10.1063/1.4801880
View online: http://dx.doi.org/10.1063/1.4801880
View Table of Contents: http://jap.aip.org/resource/1/JAPIAU/v113/i16
Published by the American Institute of Physics.

JOURNAL OF APPLIED PHYSICS **113**, 164901 (2013)

A computational analysis of graphene adhesion on amorphous silica

Eunsu Paek and Gyeong S. Hwang[a)]
Department of Chemical Engineering, University of Texas, Austin, Texas 78712, USA

(Received 25 December 2012; accepted 1 April 2013; published online 22 April 2013)

We present a computational analysis of the morphology and adhesion energy of graphene on the surface of amorphous silica (a-SiO_2). The a-SiO_2 model surfaces obtained from the continuous random network model-based Metropolis Monte Carlo approach show Gaussian-like height distributions with an average standard deviation of 2.91 ± 0.56 Å, in good agreement with existing experimental measurements (1.68–3.7 Å). Our calculations clearly demonstrate that the optimal adhesion between graphene and a-SiO_2 occurs when the graphene sheet is slightly less corrugated than the underlying a-SiO_2 surface. From morphology analysis based on fast Fourier transform, we find that graphene may not conform well to the relatively small jagged features of the a-SiO_2 surface with wave lengths of smaller than 2 nm, although it generally exhibits high-fidelity conformation to a-SiO_2 topographic features. For 18 independent samples, on average the van der Waals interaction at the graphene/a-SiO_2 interface is predicted to vary from $E_{vdW} = 0.93$ eV to 1.56 eV per unit cross-sectional area (nm^2) of the a-SiO_2 slab, depending on the choice of 12-6 Lennard-Jones potential parameters, while the predicted strain energy of corrugated graphene on a-SiO_2 is $E_{st} = 0.25$–0.36 eV/nm^2. The calculation results yield the graphene/a-SiO_2 adhesion energy of about $E_{ad} = 0.7$–1.2 eV/nm, given $E_{ad} = E_{vdW}$–E_{st}. We also discuss how the adhesive strength is affected by the morphological conformity between the graphene sheet and the a-SiO_2 surface. © *2013 AIP Publishing LLC*. [http://dx.doi.org/10.1063/1.4801880]

I. INTRODUCTION

Graphene has received great attention for potential use in a wide range of applications due to its unique physical and chemical properties.[1] For instance, graphene has been considered as a promising channel material for future electronic devices.[2] However, its electronic transport properties tend to be sensitive to the interaction with the underlying substrate; when a graphene sheet is placed on an atomically rough substrate, charge transport in graphene can be influenced by its morphological corrugation, which is dominated by the graphene-substrate adhesion.[3] Likewise, the adhesion between graphene and other materials may play an important role in determining the performance of many graphene-based devices, let alone their fabrications.

In recent years, several research groups have experimentally characterized graphene adhesion on the surface of a-SiO_2, which is an important support material for graphene in various applications.[4–8] Earlier atomic force microscopy measurements[4,5] showed evidence that highly flexible graphene can conform to a rough a-SiO_2 surface with high fidelity. While the conformal adhesion is thought be driven mainly by the van der Waals (vdW) force between graphene and a-SiO_2,[4] previous estimates for the graphene/SiO_2 adhesion energy are widely scattered. Ishigami *et al.*[4] estimated the graphene/SiO_2 interaction energy to be 0.6 eV/nm^2 based on the interlayer vdW interaction in graphite. A similar value ($\approx$0.63 eV/nm^2) was predicted by Miwa *et al.*[9] using density functional theory (DFT) calculations with vdW interaction corrections. On the other hand, the adhesion energy measured by Koenig *et al.*[8] is substantially higher, 2.81 eV/nm^2 for monolayer graphene and 1.93 eV/nm^2 for multilayer (2–5 layers) graphene. For other substrate materials, the adhesion energies of graphene on polydimethylsiloxane and copper are experimentally estimated to be 0.044 eV/nm^2 (by Scharfenberg *et al.*[10]) and 4.49 eV/nm^2 (by Yoon *et al.*[11]), respectively. The widely scattered values may be due to the difficulty of precise measurement of the adhesion strength of a single-atom-thick carbon layer particularly on an amorphous solid surface using conventional experimental techniques. In addition, the high computational cost of DFT calculations may make them limited to small structural models; for instance, the surface area of a-SiO_2 samples employed in previous DFT calculations[9,12,13] is around 1–2 nm^2, which can be insufficient to replicate properly a-SiO_2 surface roughness and in turn graphene/a-SiO_2 adhesion characteristics.

In this work, we evaluate the structure and adhesion energy of graphene on a-SiO_2 using classical force field calculations. The vdW interaction between graphene and a-SiO_2 is computed by employing three different sets of vdW parameters, which were extracted from the Charmm and Dreiding force fields and by fitting to semi-empirical dispersion corrected DFT (DFT-D2) calculations. Continuous Random Network model-based Metropolis Monte Carlo (CRN-MMC) simulations are performed to prepare defect-free a-SiO_2 surface models with various degrees of surface roughness; the a-SiO_2 surface structures are analyzed in terms of surface height distribution and Si/O spatial distribution. For different surface morphologies of a-SiO_2, we determine the topology of graphene that leads to the optimal

[a)]Author to whom correspondence should be addressed: E-mail: gshwang@che.utexas.edu

adhesion on each a-SiO_2 surface; the graphene/a-SiO_2 interface structure is used to estimate the adhesion energy (which is given in terms of the vdW interaction energy between graphene and a-SiO_2 and the strain energy of corrugated graphene on a-SiO_2). Finally, we also look at the sensitivity of the adhesive strength to the morphological conformity between graphene and a-SiO_2.

II. CALCULATION METHODS

A. Graphene/a-SiO_2 interface structure determination

As illustrated in Fig. 1, we first constructed nine (9) defect-free a-SiO_2 slabs using CRN-MMC simulations [(a) → (b)].[14] For each slab, 3600 SiO_2 units were placed in a supercell with lateral dimensions of $77.22\,\text{Å} \times 77.22\,\text{Å}$, yielding a slab thickness of about 20 Å. The top- and bottom-layer Si atoms were all passivated with O atoms, giving two defect-free surfaces. The highly strained initial structures were then relaxed via a sequence of bond transpositions using the MMC sampling based on the energetics from Keating-like potentials for silica.[14] During the geometry relaxation, two-dimensional periodic boundary conditions were imposed in the x and y directions.

Then, two single graphene sheets were placed, respectively, on the top and bottom surfaces of the a-SiO_2 slab. The initial graphene/a-SiO_2 system was relaxed using molecular dynamics (MD) at 100 K for 100 picoseconds, followed by static energy minimization using the conjugate gradient method (until the total energy change between two consecutive iterations steps became less than 10^{-5} eV) [(b) → (c) in Fig. 1]. For each system, the optimal adhesion condition was determined by varying the size (lateral dimension) of graphene. We used the AIREBO potential[15,16] for describing the structure and energetics of graphene, and refined the a-SiO_2 slab structure with the CHIK force field.[17] The 12-6 Lennard-Jones (LJ) potential was used to describe the vdW interaction between a-SiO_2 and graphene. The MD and (static) energy minimization simulations were performed using the Large-scale Atomic/Molecular Massively Parallel Simulator (LAMMPS) program.[18]

B. Van der Waals parameter selection

The predicted graphene/a-SiO_2 adhesion strength can strongly depend on the choice of vdW parameters; therefore, caution is required in selecting them. As listed in Table I, we employed three different sets of LJ parameters (σ_i, ε_i) for Si and O atoms in a-SiO_2 (which were extracted from Charmm[19] and Dreiding[20] force fields, and also by fitting to the graphene/a-SiO_2 interaction energies from semi-empirical dispersion corrected DFT calculations[21]); they are hereafter referred to as LJ(Charmm), LJ(Dreiding), and LJ(DFT-D2), respectively. The LJ parameters for C in graphene are from Ref. 22.

LJ(DFT-D2) parameters were obtained as follows. First, three a-SiO_2 slabs with 20 SiO_2 units each were constructed using combined CRN-MMC and DFT calculations,[14] and then a graphene sheet was placed on top of each slab; the a-SiO_2 lateral dimensions ($=8.544 \times 7.399$ Å^2) were adjusted to match the 24-atom rectangular graphene supercell with a lattice constant of 2.466 Å (calculated). The graphene/a-SiO_2 interaction energies were calculated by varying the distance of graphene from the a-SiO_2 surface using the DFT-D2 approach. With the DFT-D2 data, the optimal values for σ_i and ε_i were obtained through minimization of the cross-validation error (ξ); $\xi^2 = \frac{1}{N}\sum_{n=1}^{N}(E_{DFT-D2}^{(n)} - E_{LJ}^{(n)})^2$, where $E_{DFT-D2}^{(n)}$ and $E_{LJ}^{(n)}$ refer to the DFT-D2 and LJ energies, respectively, of the nth of N total data. Here, the $\varepsilon_{Si}/\varepsilon_O$ ratio was fixed at 2 as employed in LJ(Charmm). As summarized in Table I, the optimized ε_{Si} and ε_O values turn out to be substantially smaller compared to LJ(Charmm), while the σ values are close to LJ(Charmm). As such, as shown in Fig. 2, LJ(Charmm) and LJ(Dreiding) tend to overestimate the graphene/a-SiO_2 interaction compared to LJ(DFT-D2) and DFT-D2.

C. Density functional theory

Our DFT calculations were performed within the Perdew-Burke-Ernzerhof (PBE) generalized gradient approximation[23] using the Vienna *Ab initio* Simulation Package (VASP).[24] We employed the projector augmented wave (PAW) method to describe the interaction between core and valence electrons,[25] and a planewave basis set with a kinetic energy cutoff of 400 eV. Periodic boundary conditions were imposed in all three directions with a vacuum gap of 30 Å in the vertical (z) direction to separate the system from its periodic images. A $(6 \times 6 \times 1)$ k-point grid in the scheme of Monkhorst-Pack[26] was used for the Brillouin zone sampling. We used the semi-empirical approach proposed by Grimme, also known as the DFT-D2 method,[27] to take into account the vdW forces within DFT in determining the graphene/a-SiO_2 interaction energy.

III. RESULTS AND DISCUSSION

A. Surface structure of a-SiO_2

We first analyzed the atomic structure of 18 different a-SiO_2 surfaces employed in this work; note that the vdW

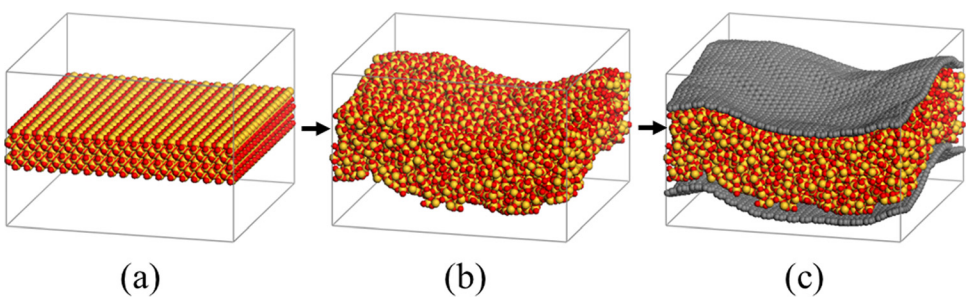

FIG. 1. (a) SiO_2 slab initial configuration, (b) defect-free a-SiO_2 slab structure constructed using the CRN-MMC approach, (c) relaxed graphene/a-SiO_2 interface structure; two single graphene sheets are, respectively, placed on the top and bottom surfaces of the a-SiO_2 slab.

TABLE I. 12-6 LJ parameters employed in this work.

	ε (eV)	σ (Å)
	Charmm/Dreiding/DFT-D2	Charmm/Dreiding/DFT-D2
S	0.01301/0.013443/0.00576	3.8264/3.8041/3.8230
O	0.00650/0.00415/0.00288	3.1181/3.0332/3.0669
C	0.00239	3.4121

interaction of graphene with the underlying a-SiO_2 surface can be a function of surface density and composition. The surface Si and O atoms were chosen such that their surface-projected coordinates have no overlap with those of other atoms nearer the surface [see the inset of Fig. 3(b)]; the overlap radii of 2.511 Å for Si and 2.252 Å for O were selected based on the projection of the average Si-Si and O-O separations.

The defect-free a-SiO_2 surfaces mostly show Gaussian-like height distributions; as summarized in Table II, the standard deviation (σ_{SiO2}) varies from 1.95 to 3.65 Å with an average of 2.91 ± 0.56 Å. The surface roughness is in good agreement with existing experimental measurements (1.68–3.7 Å)[4–8] In the surface layers, the number densities (per unit horizontal cross-sectional area) of Si and O atoms are estimated to be about $n_{Si} = 8.25 \pm 0.17\,nm^{-2}$ and $n_O = 10.92 \pm 0.25\,nm^{-2}$, yielding an Si:O ratio of 1:1.32; however, on average, O atoms are 0.62 ± 0.06 Å more protruded than Si atoms from the a-SiO_2 surface.

Figure 3 shows the radial pair distribution functions for Si-Si, Si-O, and O-O in a-SiO_2 bulk [(a)] and surface layer [(b)]. For the bulk structure with a density of 2.26 g/cm^3 (Ref. 14), the calculated first peak positions of 1.63/2.63/3.13 Å for the Si-O/O-O/Si-Si pairs are close to the corresponding experimental values of 1.62/2.65/3.12 Å.[28] In the surface layers, we notice that the first peak position of Si-Si (= 2.93 Å) noticeably decreases in comparison to that (= 3.13 Å) in the bulk, which is apparently related to the relatively high Si density compared to the bulk counterpart; while there is no noticeable change in the Si-O and O-O peak positions.

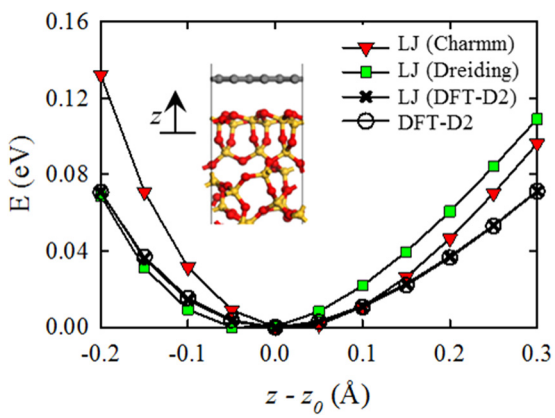

FIG. 2. Comparison of the graphene/SiO_2 interaction energies as a function of graphene-SiO_2 distance (z) from semi-empirical dispersion corrected DFT (DFT-D2) and force field calculations with different sets of 12-6 Lennard Jones (LJ) parameters (see Table I). Here, the equilibrium distance (z_0) is estimated to be around 3.58 Å.

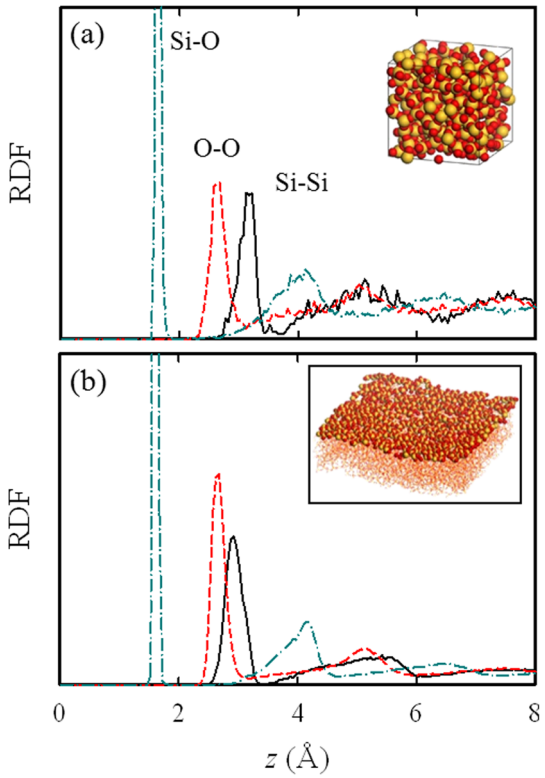

FIG. 3. Radial distribution functions (RDF) for Si-Si, Si-O, and O-O pairs in a-SiO_2 bulk [(a)] and surface layer [(b)], as illustrated in the insets.

B. Interfacial structure and adhesion strength

The structure and adhesive strength of the graphene/a-SiO_2 interface were calculated by varying the size (lateral dimension) of graphene; special care was taken to ensure that the graphene sheet was conformally adhered to the rough a-SiO_2 surface. Once the optimal topology of graphene was determined, the graphene/a-SiO_2 adhesion energy was estimated using

$$E_{ad} = -\frac{1}{A}(E_{Gr/SiO_2} - E_{SiO_2} - N_C\overline{E}_{Gr}),$$

where, E_{Gr/SiO_2} and E_{SiO_2} are the total energies of the graphene/a-SiO_2 system and the a-SiO_2 slab, respectively, $\overline{E}_{Gr}$ is the per-atom energy of pristine graphene, N_C is the number of C atoms in the adhered graphene sheet, and A is the a-SiO_2 slab cross-sectional area.

The interface strength is also often characterized by the work of separation (W_{sp}), which represents the reversible work required to separate the interface into two free surfaces; that is, $W_{sp} = -(E_{Gr/SiO_2} - \mathring{E}_{SiO_2} - \mathring{E}_{Gr})/A$, where $\mathring{E}_{SiO_2}$ and $\mathring{E}_{Gr}$ refer to the total energies of the a-SiO_2 slab and the corrugated graphene sheet attached to the a-SiO_2 surface, respectively, with no relaxation after separation. Note that E_{ad} differs from W_{sp} in that it takes full account of structural relaxation after separation. In our calculations, the a-SiO_2 slab energy is found to merely change before and after the relaxation (i.e., $E_{SiO_2} \approx \mathring{E}_{SiO_2}$) and the energy of corrugated graphene can be described in terms of its elastic strain energy (E_{st}). Therefore, for the graphene/a-SiO_2 interface, E_{ad} can be approximated by W_{sp} minus E_{st}. In addition, given

TABLE II. Standard deviations (σ) of surface height distributions of graphene and a-SiO_2, graphene-SiO_2 distances ($d_{Gr\text{-}SiO_2}$), and graphene-SiO_2 van der Waals interaction energies (E_{vdW}), and graphene strain energies (E_{st}), calculated using three different sets of LJ parameters (see Table I); the three values are given in the order of LJ(DFT-D2)/LJ(Charmm)/LJ(Dreiding).

	σ			
a-SiO_2 (Å)	Graphene (Å)	$d_{Gr\text{-}SiO_2}$ (Å)	E_{vdW} (eV/nm^2)	E_{st} (eV/nm^2)
1.95	1.88/1.80/1.81	4.13/3.94/3.92	0.95/1.57/1.41	0.19/0.29/0.28
2.00	1.93/1.84/1.85	4.16/3.96/3.99	0.97/1.60/1.40	0.21/0.30/0.25
2.26	2.18/2.11/2.08	4.36/4.20/4.14	0.93/1.50/1.36	0.24/0.31/0.33
2.32	2.09/2.09/2.08	4.17/3.99/4.00	0.94/1.55/1.37	0.18/0.27/0.23
2.53	2.29/2.27/2.26	4.13/3.95/4.01	0.96/1.57/1.36	0.17/0.26/0.21
2.59	2.25/2.30/2.28	4.32/4.07/4.10	0.92/1.56/1.37	0.25/0.38/0.34
2.63	2.31/2.24/2.22	4.15/3.93/3.98	0.95/1.57/1.38	0.19/0.30/0.26
2.71	2.36/2.36/2.36	4.21/3.98/4.09	0.94/1.57/1.34	0.23/0.35/0.27
2.77	2.19/2.21/2.22	4.27/4.13/4.07	0.90/1.45/1.32	0.23/0.30/0.30
2.77	2.25/2.24/2.33	4.00/3.71/4.05	1.00/1.67/1.35	0.21/0.34/0.16
3.21	2.47/2.51/2.50	4.58/4.33/4.32	0.84/1.42/1.27	0.22/0.32/0.30
3.33	3.18/3.13/3.14	4.21/3.98/3.97	0.99/1.64/1.46	0.44/0.56/0.52
3.46	3.20/3.21/3.21	4.08/3.92/3.89	1.01/1.66/1.49	0.40/0.50/0.49
3.53	2.85/3.42/3.45	5.03/4.16/4.10	0.76/1.60/1.44	0.14/0.48/0.49
3.53	3.30/3.26/3.28	4.27/4.10/4.08	0.98/1.62/1.44	0.38/0.47/0.46
3.55	2.98/3.08/3.09	4.34/4.06/4.19	0.87/1.48/1.25	0.19/0.31/0.23
3.61	2.99/3.04/3.09	4.39/4.11/4.19	0.81/1.39/1.20	0.14/0.27/0.22
3.65	3.28/3.26/3.26	4.21/3.97/3.96	1.00/1.67/1.48	0.43/0.55/0.52
2.91 ± 0.56	2.55 ± 0.47/ 2.57 ± 0.53/ 2.58 ± 0.53	4.28 ± 0.22/ 4.03 ± 0.13/ 4.06 ± 0.10	0.93 ± 0.07/ 1.56 ± 0.08/ 1.37 ± 0.08	0.25 ± 0.09/ 0.36 ± 0.10/ 0.32 ± 0.11

that the interfacial adhesion is entirely due to the vdW force, W_{sp} should be equal to the vdW interaction energy (E_{vdW}) such that E_{ad} is given in terms of E_{vdW} and E_{st} (i.e., $E_{ad} = E_{vdW} - E_{st}$).

We evaluated the vdW interaction at the interface using three different sets of LJ parameters [LJ(DFT-D2), LJ(Charmm), LJ(Dreiding)] and the elastic strain of corrugated graphene with the AIREBO potential. From the 18 independent interface structures considered, the predicted E_{vdW} values vary from 0.93 ± 0.07 eV/nm^2 [LJ(DFT-D2)], 1.37 ± 0.08 eV/nm^2 [LJ(Dreiding)] to 1.56 ± 0.08 eV/nm^2 [LJ(Charmm)]. Since a stronger vdW interaction at the graphene/a-SiO_2 interface causes the graphene sheet to be more corrugated, the predicted E_{st} becomes largest ($= 0.36 \pm 0.10$ eV/nm^2) with LJ(Charmm), followed by 0.32 ± 0.11 eV/nm^2 [LJ(Dreiding)] and 0.25 ± 0.09 eV/nm^2 [(DFT-D2)]. As a result, E_{ad} ($= E_{vdW} - E_{st}$) is predicted to be 0.68 eV/nm^2 (DFT-D2), 1.05 eV/nm^2 (Dreiding), and 1.20 eV/nm^2 (Charmm). Our predicted adhesion energies are within the range of 0.6/0.63–2.81 eV/nm^2 as reported by previous studies.[4,8,9]

As illustrated in Fig. 4, the height distribution comparison between graphene and SiO_2 clearly shows that the optimal graphene/a-SiO_2 adhesion commonly occurs when the graphene sheet is slightly less corrugated than the underlying a-SiO_2 surface, consistent with previous experiments.[5,6] For the 18 model interface systems considered, the predicted σ_{Gr} and σ_{SiO_2} with LJ(DFT-D2) are 2.55 ± 0.47 Å and 2.91 ± 0.56 Å, respectively; here, the average graphene-SiO_2 distance is predicted to be $d_{Gr\text{-}SiO_2} = 4.28 \pm 0.22$ Å, which is very close to the experimental value of 4.2 Å.[4] The average value of $d_{Gr\text{-}SiO_2}$ decreases to 4.03/4.06 Å when using LJ(Charmm)/LJ(Dreiding), due to the increased vdW forces; however, the topological change of graphene appears to be insignificant with the choice of LJ parameter sets (i.e., σ_{Gr} only varies from 2.55 Å to 2.58 Å). It is also worth noting that there is an insignificant variance in $d_{Gr\text{-}SiO_2}$, although the surface roughness of a-SiO_2 varies significantly from sample to sample; this is apparently due to the fact that graphene is highly flexible and complies well with the morphological change of the underlying a-SiO_2 surface.

For comparison, we also estimated the E_{st} of corrugated graphene using[29]

$$E_{st} = \frac{C}{2}\left\{\frac{1}{S}\int [\nabla^2 h(r)]^2 d^2 r\right\}, \quad (1)$$

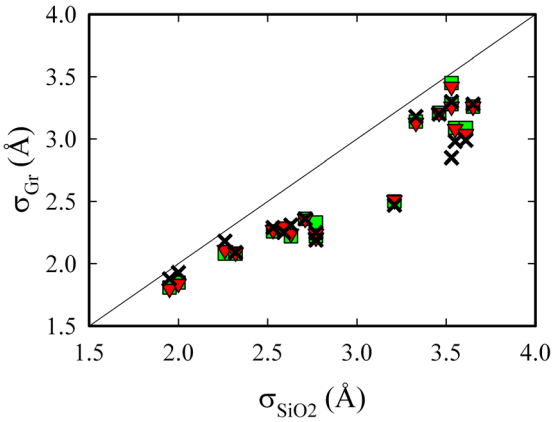

FIG. 4. Predicted standard deviations of height distributions of graphene (σ_{Gr}) with respect to the corresponding a-SiO_2 surface (σ_{SiO_2}) for three different sets of LJ parameters employed.

where C is the bending rigidity of graphene, S is the integration domain area, and $h(r)$ is the local height of graphene at the spatial position r. A corrugated graphene sheet was mapped into a rectangular grid for the integration with a careful selection of optimal grid size (≈1.6 Å). For the same graphene topologies as obtained with AIREBO/DFT-D2 (*vide supra*), E_{st} is predicted to be 0.17–0.30 eV/nm^2 for a typical range of $C = 0.85$-1.5 eV,[30–32] which is in good agreement with $E_{st} = 0.25 \pm 0.09$ eV/nm^2 as estimated with the AIREBO potential. Our calculations clearly demonstrate that the E_{vdW} between graphene and a-SiO_2 can be substantially greater than the E_{st} associated with the resulting corrugation of graphene, permitting high-fidelity topological conformation of graphene to the rough surface of a-SiO_2.

C. Morphological conformity effect

Next, we turned to examining how the adhesive strength is affected by the morphological conformity between graphene and a-SiO_2. Figure 5 shows the variations of E_{vdW} and $d_{Gr\text{-}SiO_2}$ with σ_{Gr} (which can be used as a measure of the extent of graphene corrugation); a smaller (larger) value of σ_{Gr} indicates that the graphene sheet is less (more) corrugated as shown in the upper panels [(A)–(C)]. In this case, the optimal adhesion is achieved when the graphene sheet is slightly less corrugated ($\sigma_{Gr} = 3.28$ Å) than the underlying a-SiO_2 surface ($\sigma_{SiO_2} = 3.65$ Å, indicated as the dashed line). The calculation results clearly show that E_{vdW} drops rapidly as σ_{Gr} increases or decreases relative to the optimal case ($\sigma_{Gr} = 3.28$ Å); the reduced vdW interaction is apparently attributed to the decreased graphene/a-SiO_2 contact area. Likewise, $d_{Gr\text{-}SiO_2}$ is found to increase as the graphene sheet adheres less conformally to the a-SiO_2 surface.

We also performed Fast Fourier Transform (FFT) analysis to evaluate the degree of the topological conformity of graphene to a-SiO_2 for various σ_{Gr}. When $\sigma_{Gr} = 3.28$ Å (optimal adhesion), as shown in Fig. 6(a), the Fourier amplitudes of graphene and a-SiO_2 are nearly identical when the wave length (λ) is greater than 2 nm. However, for $\lambda < 2$ nm, we can see a noticeable discrepancy between the graphene and a-SiO_2 spectra, implying that the graphene sheet may not conform well to the relatively small jagged features of the a-SiO_2 surface. The three-dimensional (3-D) mesh surface plots (insets) of graphene and a-SiO_2 also clearly demonstrate that graphene replicates well the surface topology of a-SiO_2, except the rough localized features with small

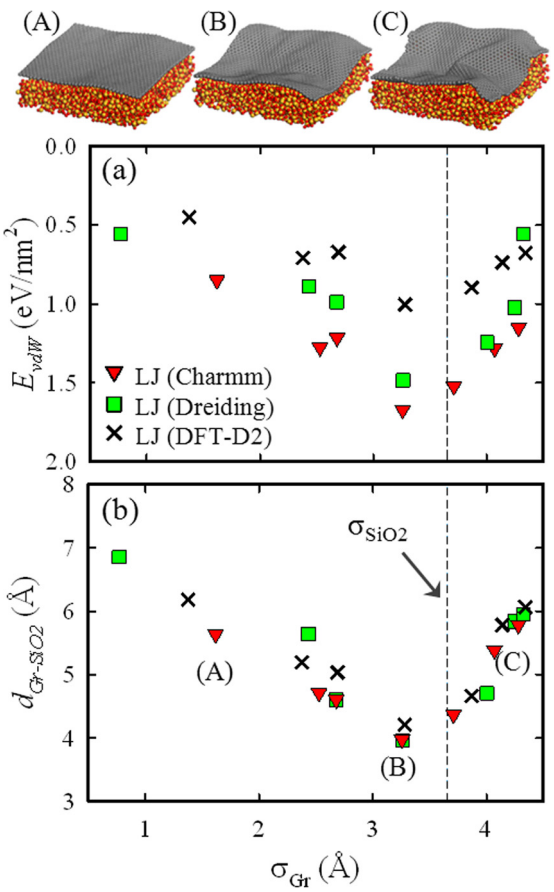

FIG. 5. Variations in the graphene/a-SiO_2 vdW interaction energy (E_{vdW}) and distance ($d_{Gr\text{-}SiO_2}$) as a function of the standard deviation of graphene height distributions (σ_{Gr}); here, only one a-SiO_2 surface with $\sigma_{SiO_2} = 3.65$ Å (indicated as the vertical dashed line) was used. Three selected graphene/a-SiO_2 interface structures [(A)–(C) as indicated in (b)] are shown in the upper panels.

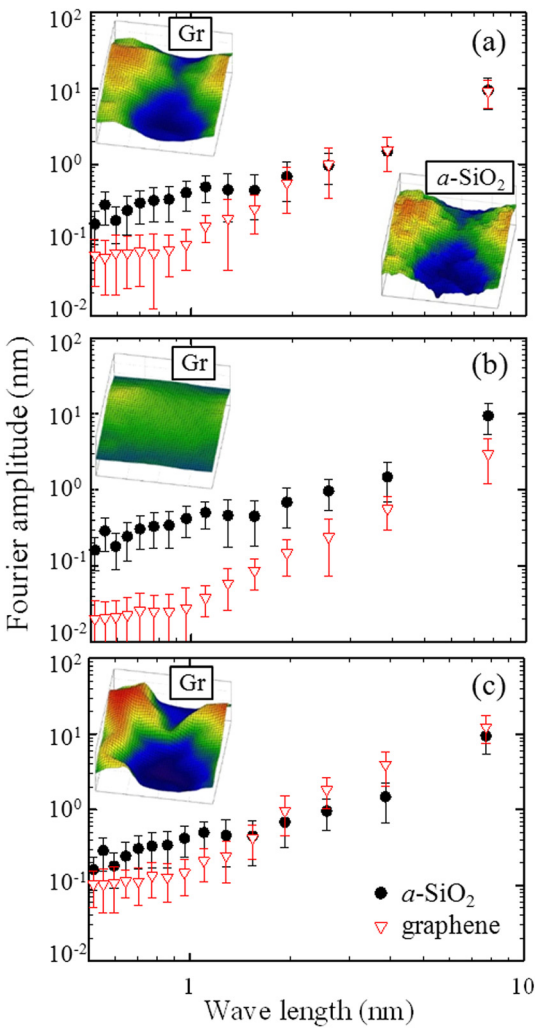

FIG. 6. Fast Fourier transform of graphene and a-SiO_2 surface morphologies for three different adhesion conditions; (a) optimal, (b) less corrugated, and (c) more corrugated. Corresponding surface contour plots are also shown as insets.

curvatures. This implies that the energy cost for conforming to the very bumpy features may exceed the energy gain from the consequently increased graphene/a-SiO_2 contact area. A back-of-the-envelope calculation based on Hook's law also suggests that graphene may hardly conform to a rough surface (which has radii of curvature less than 1.0–1.3 nm (Ref. 33)).

If the graphene sheet is much less [Fig. 6(b)] or more [Fig. 6(c)] corrugated than the a-SiO_2 surface, as expected, there are significant discrepancies in the Fourier amplitudes over almost the entire range of wavelengths. At $\sigma_{Gr} = 1.62$ Å [Fig. 6(b)], the graphene amplitude is consistently lower than the a-SiO_2 case, indicating that the graphene sheet remains relatively flat. On the other hand, when $\sigma_{Gr} = 4.28$ Å [Fig. 6(c)], above 2 nm (in λ), the amplitude of graphene gets larger than that of a-SiO_2, which is apparently due to the more corrugated graphene; still the graphene sheet cannot conform to the small/localized roughness features ($\lambda < 2$ nm) of the a-SiO_2 surface. For both cases [Figs. 6(b) and 6(c)], compared to the optical adhesion case [Fig. 6(a)], E_{ad} significantly decreases while $d_{Gr\text{-}SiO_2}$ increases because of the reduced graphene/a-SiO_2 vdW interaction.

IV. SUMMARY

Classical force field calculations were performed to evaluate the morphology and adhesion energy of graphene on the surface of a-SiO_2. First, nine (9) independent defect-free a-SiO_2 slabs were constructed CRN-MMC simulations, providing eighteen (18) surface models with different degrees of roughness. We find that the a-SiO_2 surfaces mostly show Gaussian-like height distributions; the standard deviation varies from 1.95 to 3.65 Å with an average of 2.91 ± 0.56 Å, in good agreement with existing experimental measurements (1.68–3.7 Å). In the silica surface layers, the number densities (per unit horizontal cross-sectional area) of Si and O atoms are predicted to be about $n_{Si} = 8.25 \pm 0.17\,nm^{-2}$ and $n_O = 10.92 \pm 0.25\,nm^{-2}$, while on average O atoms are 0.62 ± 0.06 Å more protruded than Si atoms from the a-SiO_2 surface.

Based on the a-SiO_2 surface models, the adhesion of graphene was examined by employing three different sets of LJ parameters (which were extracted from Charmm and Dreiding force fields and also by fitting to semi-empirical dispersion corrected DFT results). While the optimal adhesion tends to occur when the graphene sheet is slightly less corrugated than the underlying a-SiO_2 surface, the predicted vdW interaction at the interface (E_{vdW}) varies from 0.93 ± 0.07 [LJ(DFT-D2)], 1.37 ± 0.08 [LJ(Dreiding)] to $1.56 \pm 0.08\,eV/nm^2$ [LJ(Charmm)]. Since a stronger interfacial interaction causes the graphene sheet to be more corrugated, the strain energy in graphene (E_{st}) turns out to be largest ($= 0.36 \pm 0.10\,eV/nm^2$) with LJ(Charmm), followed by $0.32 \pm 0.11\,eV/nm^2$ [LJ(Dreiding)] and $0.25 \pm 0.09\,eV/nm^2$ [(DFT-D2)]. From the results, the graphene/a-SiO_2 adhesion energy ($E_{ad} = E_{vdW} - E_{st}$) is estimated to be $0.68–1.20\,eV/nm^2$, depending on the choice of LJ parameters. We also find that the adhesive strength is rather sensitive to the morphological conformity between graphene and a-SiO_2; that is, E_{vdW} drops rapidly as graphene is more (or less) corrugated compared to the optimal adhesion case, which is attributed to the decreased graphene/a-SiO_2 contact area. Finally, morphology analysis based on Fast Fourier Transform clearly demonstrates that, in general, highly flexible graphene is easily corrugated to follow the underlying rough a-SiO_2 surface, but does not conform well to relatively small jagged features with wave lengths of smaller than 2 nm.

ACKNOWLEDGMENTS

We acknowledge National Science Foundation (CBET-0933557) and Robert A. Welch Foundation (F-1535) for their financial support. We would also like to thank the Texas Advanced Computing Center for use of their computing resources.

[1]K. S. Novoselov, D. Jiang, F. Schedin, T. J. Booth, V. V. Khotkevich, S. V. Morozov, and A. K. Geim, Proc. Natl. Acad. Sci. U.S.A. **102**, 10451 (2005).
[2]F. Schwierz, Nat. Nanotechnol. **5**, 487 (2010).
[3]M. I. Katsnelson and A. K. Geim, Philos. Trans. R. Soc. London, Ser. A **366**, 195 (2008).
[4]M. Ishigami, J. H. Chen, W. G. Cullen, M. S. Fuhrer, and E. D. Williams, Nano Lett. **7**, 1643 (2007).
[5]C. H. Lui, L. Liu, K. F. Mak, G. W. Flynn, and T. F. Heinz, Nature **462**, 339 (2009).
[6]W. Cullen, M. Yamamoto, K. Burson, J. Chen, C. Jang, L. Li, M. Fuhrer, and E. Williams, Phys. Rev. Lett. **105**, 215504 (2010).
[7]V. Geringer, M. Liebmann, T. Echtermeyer, S. Runte, M. Schmidt, R. Rückamp, M. Lemme, and M. Morgenstern, Phys. Rev. Lett. **102**, 076102 (2009).
[8]S. P. Koenig, N. G. Boddeti, M. L. Dunn, and J. S. Bunch, Nat. Nanotechnol. **6**, 543 (2011).
[9]R. H. Miwa, T. M. Schmidt, W. L. Scopel, and A. Fazzio, Appl. Phys. Lett. **99**, 163108 (2011).
[10]S. Scharfenberg, D. Z. Rocklin, C. Chialvo, R. L. Weaver, P. M. Goldbart, and N. Mason, Appl. Phys. Lett. **98**, 091908 (2011).
[11]T. Yoon, W. C. Shin, T. Y. Kim, J. H. Mun, T.-S. Kim, and B. J. Cho, Nano Lett. **12**, 1448 (2012).
[12]Z. Ao, M. Jiang, Z. Wen, and S. Li, Nanoscale Res. Lett. **7**, 158 (2012).
[13]A. Rudenko, F. Keil, M. Katsnelson, and A. Lichtenstein, Phys. Rev. B **84**, 085438 (2011).
[14]S. Lee, R. J. Bondi, and G. S. Hwang, Phys. Rev. B **84**, 045202 (2011).
[15]S. J. Stuart, A. B. Tutein, and J. A. Harrison, J. Chem. Phys. **112**, 6472 (2000).
[16]D. W. Brenner, O. A. Shenderova, J. A. Harrison, S. J. Stuart, B. Ni, and S. B. Sinnott, J. Phys. Condens. Matter **14**, 783 (2002).
[17]A. Carfe, J. Horbach, S. Ispas, and W. Kob, Europhys. Lett. **82**, 17001 (2008).
[18]S. Plimpton, J. Comput. Phys. **117**, 1 (1995).
[19]E. R. Cruz-Chu, A. Aksimentiev, and K. Schulten, J. Phys. Chem. B **110**, 21497 (2006).
[20]S. L. Mayo, B. D. Olafson, and W. A. Goddard III, J. Phys. Chem. **94**, 8897 (1990).
[21]X. Wu, M. C. Vargas, S. Nayak, V. Lotrich, and G. Scoles, J. Chem. Phys. **115**, 8748 (2001).
[22]L. A. Girifalco, M. Hodak, and R. S. Lee, Phys. Rev. B **62**, 13104 (2000).
[23]J. P. Perdew, K. Burke, and M. Ernzerhof, Phys. Rev. Lett. **77**, 3865 (1996).
[24]G. Kresse and J. Furthmuller, *VASP the Guide* (Vienna University of Technology, Vienna, 2001).
[25]P. E. Blöchl, Phys. Rev. B **50**, 17953 (1994).
[26]H. J. Monkhorst and J. D. Pack, Phys. Rev. B **13**, 5188 (1976).
[27]S. Grimme, J. Comput. Chem. **27**, 1787 (2006).
[28]R. L. Mozzi and B. E. Warren, J. Appl. Cryst. **2**, 164 (1969).
[29]G. Palasantzas and G. Backx, Phys. Rev. B **54**, 8213 (1996).
[30]B. I. Yakobson, C. J. Brabec, and J. Bernholc, Phys. Rev. Lett. **76**, 2511 (1996).

[31]A. Incze, A. Pasturel, and P. Peyla, Phys. Rev. B **70**, 212103 (2004).
[32]K. N. Kudin, G. E. Scuseria, and B. I. Yakobson, Phys. Rev. B **64**, 235406 (2001).
[33]The E_{st} of Gr due to bending can be calculated using a simple formula for bending energy ($E_b = {}^1/_2 C\kappa^2$, where κ is the curvature and C is bending rigidity). In order to explore this, the E_b term is substituted to E_{vdW} ($= 0.93$ eV/nm^2) in the uniaxial bending energy formula. When C is bounded at 0.85–1.5 eV, it is found that graphene would be off when D $<$ 1.9–2.5 nm. Here, D is the diameter of the rough feature for symmetric biaxial bending.